J Inorg Organomet Polym (2013) 23:751–757
DOI 10.1007/s10904-012-9807-4

COMMUNICATION

New Flower-Shaped Lead(II) Coordination Polymer at the Nano Scale: Synthesis, Structural Characterization and DFT Calculations of $[Pb(o\text{-phen})(N_3)_2]_n$ Containing the Pb-($\mu_{1,1}$-N_3)($\mu_{1,3}$-N_3) Motif

Babak Mirtamizdoust · Safa Ali-Asgari · Sang Woo Joo · Ehsan Maskani · Younes Hanifehpour · Tae Hwan Oh

Received: 18 September 2012 / Accepted: 5 December 2012 / Published online: 13 December 2012

Abstract A new nano-flower lead(II) azido coordination polymer from the ligand, orthophenanthroline (*o*-phen), $[Pb(o\text{-phen})(\mu_{1,1}\text{-}N_3)(\mu_{1,3}\text{-}N_3)]_n$ (**1**), was synthesized by a sonochemical method. Compound **1** was characterized by scanning electron microscopy (SEM), X-ray diffraction (XRD), elemental analyses and IR spectroscopy. Single crystalline material was obtained using a heat gradient applied to a solution of the reagents. The structure of **1** is a coordination polymer of lead(II) containing the Pb-($\mu_{1,1}$-N_3)($\mu_{1,3}$-N_3) motif, formed of one-dimensional chains. The structure of the **1** was optimized by density functional theory. Structural parameters and IR spectra for **1** are consistent with the crystal structure. Pure phase PbO nanoparticles were obtained by thermolysis of **1** with oleic acid as a surfactant at 180 and 200 °C an air. PbO nanoparticles were characterized by XRD and SEM.

B. Mirtamizdoust (✉) · S. W. Joo (✉) · Y. Hanifehpour
WCU Nano Research Center, School of Mechanical Engineering, Yeungnam University, Gyeongsan 712-749, South Korea
e-mail: tamizdoust@tabrizu.ac.ir

S. W. Joo
e-mail: swjoo1@gmail.com

B. Mirtamizdoust · Y. Hanifehpour
Inorganic Compounds Research Laboratory, Faculty of Chemistry, University of Tabriz, 51666-16471 Tabriz, Iran

S. Ali-Asgari · E. Maskani
Department of Chemistry, Shahrood Branch, Islamic Azad University, 36155/133 Shahrood, Iran

T. H. Oh
Department of Nano, Medical and Polymer Materials, Yeungnam University, Gyeongsan 712-749, South Korea

Keywords Nano coordination polymer · Nano oxide · Lead(II) · DFT

1 Introduction

The design and construction of nano-materials are an important area of research, especially because of the physical and chemical properties of these materials that depend on particle size. The properties of inorganic nano-materials strongly depend on particle morphology, thus making the design and controlled large-scale synthesis of nano-structures with different morphological configurations and size distributions very important for basic science and technological applications [1–5]. Coordination polymers are widely studied and are an important frontier in polymer and coordination chemistry. In the last decade, coordination compounds with infinite one-, two-, and three-dimensional network structures have been reported [6].

Research into coordination polymers has rapidly grown in recent years due to an increasing demand for functional materials with conductive, magnetic, non-linear optical, porous, thermal, and fluorescent properties [7–13].

In contrast to inorganic materials, the specific synthesis of nano-structured coordination polymers seems to be surprisingly sparse. Until recently, there have been only very few reports of the synthesis and properties of nano-materials made of coordination polymers [14–25]. Nano-scaled materials often exhibit new, interesting, size-dependent physical and chemical properties that cannot be observed in their bulk form. Some recent studies on nano-scale coordination polymers have been reported [26].

Sonochemistry is a research area in which molecules undergo a chemical reaction due to the application of powerful ultrasound radiation (20 kHz–10 MHz) [1, 27].

The application of ultrasound in synthetic organic chemistry has become important because ultrasonic waves in liquids were discovered to cause chemical reactions both in homogeneous and heterogeneous systems [19, 28].

In this report, we focus our attention on the design and synthesis nano-coordination compounds. We have recently reported nano-lead(II) coordination polymers [20–25]. As a continuation of our previous studies, we wish to report the simple synthesis of a nano-flowered structure of a new Pb(II)-azido one-dimensional coordination polymer, $[Pb(o\text{-phen})(\mu_{1,1}\text{-}N_3)(\mu_{1,3}\text{-}N_3)]_n$ (**1**) and its conversion to a nano-structured lead oxide by calcination at moderately elevated temperatures. The electronic structure was supported by the density functional theory (DFT) method. DFT is sufficiently accurate, easy to use and fast in the study of relatively large metal complexes [29]. DFT can also be used for geometry optimization and the calculation of spectral properties.

2 Experimental

2.1 Materials and Physical Property Measurements

All reagents and solvents for the synthesis and analysis were obtained from Sigma-Aldrich and were used as received. A multiwave ultrasonic generator (Sonicator_3000; Misonix, Inc., Farmingdale, NY, USA) was used. IR spectra were recorded using Perkin–Elmer 597 and Nicolet 510P spectrophotometers.

Microanalyses were carried out using a Heraeus CHN-O-Rapid analyzer. Melting points were measured on an Electrothermal 9100 apparatus and are uncorrected. The thermal behavior was measured with a PL-STA 1500 apparatus. X-ray powder diffraction (XRD) measurements were performed using a Philips diffractometer manufactured by X'pert with monochromatized Cu Kα radiation ($\lambda = 1.54187$ Å) and simulated XRD powder patterns based on single crystal data were prepared using mercury [17]. The crystallite sizes of selected samples were estimated using the Scherrer method. The samples were characterized by scanning electron microscopy using a gold coating. The molecular structure plots were prepared using mercury [30] and ORTEPIII [31]. The geometry of the $[Pb(o\text{-phen})(\mu_{1,1}\text{-}N_3)(\mu_{1,3}\text{-}N_3)]_n$ complex was optimized using the B3LYP density functional model [32, 33]. In these calculations, the 3-21G* basis set for C- and H-atoms was used, while the 6-31G* basis set was used for N-atoms. For Pb atoms, the LanL2DZ valence and effective core potential functions were used [34, 35]. All DFT calculations were performed using the Gaussian 98 R-A.9 package [36]. X-ray structures were used as input geometries when available.

Caution Although we have experienced no problems with the compounds reported in this work, sodium azide and azide complexes are potentially explosive and should be handled in small quantities and with great caution.

2.2 Synthesis of $[Pb(o\text{-phen})(\mu_{1,1}\text{-}N_3)(\mu_{1,3}\text{-}N_3)]_n$ (**1**)

To prepare the nano-flower structure of $[Pb(o\text{-phen})(\mu_{1,1}\text{-}N_3)(\mu_{1,3}\text{-}N_3)]_n$ (**1**), a solution of $Pb(CH_3COO)_2$ (25 mL, 0.01 M) and a solution of sodium azide (25 mL, 0.02 M) in water were positioned in a high-density ultrasonic probe. *O*-phen (25 mL, 0.01 M) in MeOH/water was added dropwise. At the end of the titration the solution remained in the bath for a selected aging time at a selected temperature. The obtained precipitates were filtered, washed with water and air dried. Product **1**: m.p. = 278 °C. Elem. Anal.: calculated (%) for $C_{24}H_{16}N_{16}Pb_2$ (**1**): C, 30.54; H, 1.69; N, 23.75; found: C, 30.45; H, 1.70; N, 24.05. IR (cm^{-1}) selected bands: 683m, 1470s, 1505, 1579s, 2040vs, 2050s, 3055w [37]. To isolate single crystals of **1**, orthophenanthroline (1 mmol) was placed in one arm of a branched tube and $Pb(CH_3COO)_2$ (1 mmol) and sodium azide (1 mmol) in the other arm. Methanol was then carefully added to fill both arms. The tube was sealed and the ligand-containing arm was immersed in a bath at 60 °C, while the other was left at ambient temperature. After 2 weeks, crystals suitable for X-ray structure determination deposited in the arm at ambient temperature. The crystals were filtered, washed with acetone and ether, and air dried; m.p. = 275 °C, Yield: 70 %. Elem. anal: Calcd. (%) for $C_{24}H_{16}N_{16}Pb_2$ (**1**): C, 30.54; H, 1.69; N, 23.75; found: C, 30.55; H, 1.72; N, 24.00. IR (cm^{-1}), selected bands: 683m, 1470s, 1505, 1579s, 2040vs, 2050s, 3050w [37].

3 Results and Discussion

Sonochemistry is an elegant approach for the synthesis of nanomaterials [11]. In this method, molecules are promoted to form nano-sized particles by the application of powerful ultrasound radiation (20 kHz–10 MHz) [38], mostly by the instantaneous formation of a plethora of crystallization nuclei. The reaction between *o*-phen with lead(II) acetate and sodium azide led to the formation **1**. Nano-flowers of **1** were obtained by ultrasonic irradiation in a water/methanolic solution. Single crystalline material was obtained using a heat gradient applied to a solution of the reagents (branched tube method). Scheme 1 gives an overview methods used by the two different routes.

The elemental analysis, IR spectra and single crystalline material are indistinguishable. The IR spectra display characteristic absorption bands for *o*-phen and azide. The strong doublet absorption band centered at ca. 2,040–2,050 cm^{-1} is

Scheme 1 Synthesis scheme

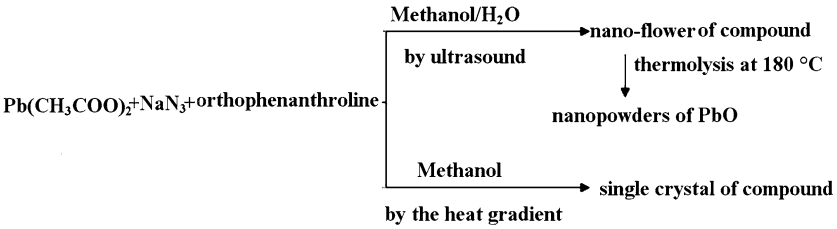

assigned to the ν_{asy} (N_3^-). This reflects the bonding mode of N_3^- as end-on ($\mu_{1,1}$) [29]. The relatively weak band at 3,050 cm^{-1} is attributed to aromatic CH hydrogens [29].

The simulated and experimental XRD patterns for **1** (Fig. 1a, b respectively), indicate acceptable matches with only slight differences in 2θ observed. This indicates that the compound obtained is a single crystalline phase and this phase is identical to that obtained by single crystal diffraction. The significant broadening of the peaks indicates that the particles are nanometer in size. Estimated by the Scherrer formula ($D = 0.891\lambda/\beta\cos$) where D is the average grain size, λ the X-ray wavelength (0.15405 nm), and θ and β are the diffraction angle and full-width at half maximum of an observed peak, gives a value of $D = 37$ nm.

The morphology of **1** prepared by the sonochemical method (Fig. 2) indicates a flower-like structure with a thickness of $\sim$37 nm (Fig. 2). The mechanism of formation of this network structure requires further investigation.

The determination of the structure of **1** by X-ray crystallography (Table 1) shows that the complex crystallizes in the triclinic system with a $P\bar{1}$ space group. In the solid state **1** is a 1D coordination polymer [39–45]. The molecular structure of the asymmetric unit with atom labeling is shown in Fig. 3. Table 2 shows the experimental and theoretical values (DFT) of the bonds lengths.

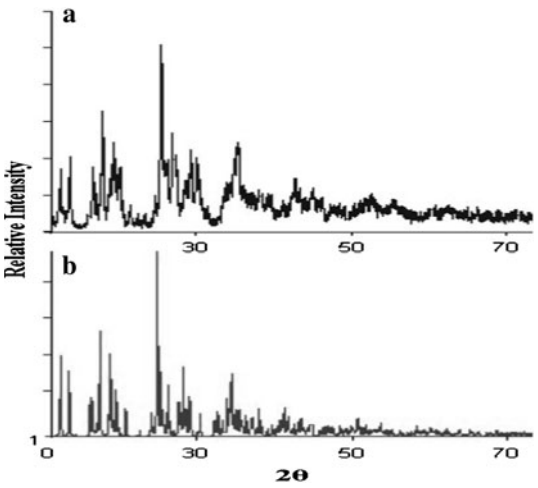

Fig. 1 The XRPD patterns; **a** computed from the single crystal X-ray data of compound **1**, **b** nano-structure of **1**

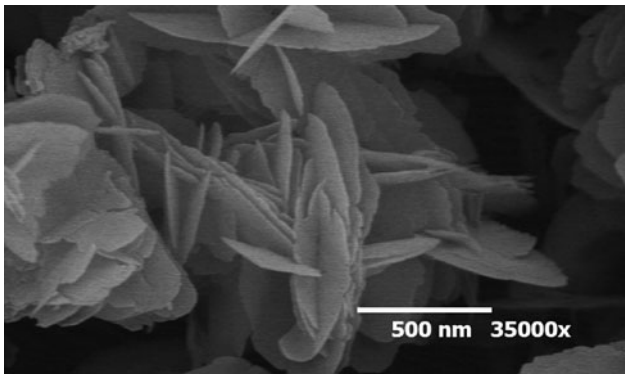

Fig. 2 SEM photographs of **1**

The coordination number of each Pb(II) atoms in **1** is six. Each lead atom is chelated by two N-atoms of a *o*-phen ligand with Pb–N distances of 2.506(6) and 2.514(5) Å. In addition, there are four N-atoms in the azide anions with Pb–N distances of 2.418(6), 2.611(6), 2.706(5) and 2.816(5) Å (Fig. 4).

The arrangement of these ligands suggests a gap or hole in the coordination geometry around the metal ions ($N8^i$–Pb1–$N3^i$ angle is 131.71(19)), possibly occupied by a stereoactive lone pair of electrons on lead(II) [46]. The observed shortening of the Pb–N bonds on the side of the Pb(II) ion opposite the putative lone pair (2.418(6) Å compared to 2.816(5) Å adjacent to the lone pair) supports this point [47]. Hence, the geometry of the nearest coordination environment of every lead atom is likely caused by the geometrical constraints of the coordinated *o*-phen ligands, azide anions and the influence of a stereochemically active lone pair of electrons in a hybrid orbital on the metal atom. Such an environment leaves space for bonding with nitrogen atoms of the azide anion of an adjacent molecule. To find any potential donor center within this vacancy, it is necessary to extend the bonding limit to at least 3.5 Å [48]. It is possible to find azide–N atoms approaching each Pb (Pb1···N5 = 3.503 Å); thus, the Pb^{II} coordination sphere is almost complete and the coordination number for **1** becomes seven (PbN7) with holodirected geometry [46]. In fact, there are two different types of coordination mode of the azide anions ($\mu_{1,1}$ and $\mu_{1,3}$) that are common for azides. Thus, each lead atom has three neighboring lead atoms bridged by azide ligands. The

Table 1 Crystal data and structure refinement for [Pb(*o*-phen)($\mu_{1,1}$-N_3)($\mu_{1,3}$-N_3)]$_n$

Empirical formula	$C_{24}H_{16}N_{16}Pb_2$
Formula weight	942.91
Temperature/K	373(2)
Crystal system	Triclinic
Space group	*P*-1
a/Å	7.5354(2)
b/Å	9.3621(2)
c/Å	9.7440(2)
α/°	89.412(1)
β/°	69.748(1)
γ/°	74.415(1)
Volume/Å^3	639.67(3)
Z	1
ρ_{calc} mg/mm^3	2.448
m/mm^{-1}	13.194
F(000)	436.0
Crystal size/mm^3	0.68 × 0.49 × 0.16
2θ range for data collection	4.54–65°
Index ranges	$-11 \le h \le 11$, $-14 \le k \le 14$, $-14 \le l \le 14$
Reflections collected	13,697
Independent reflections	4,460[*R*(int) = 0.0442]
Data/restraints/parameters	4,460/0/190
Goodness-of-fit on F^2	1.105
Final *R* indexes [$I \ge 2\sigma(I)$]	$R_1 = 0.0592$, $wR_2 = 0.1544$
Final *R* indexes [all data]	$R_1 = 0.0599$, $wR_2 = 0.1554$
Largest diff. peak/hole/*e* Å^{-3}	7.46/−4.46

Pb···Pb distance through the EO azide bridges is 4.206 Å, and that through the EE azide is 5.524 and 7.635 Å along the *b* and *a* directions, respectively.

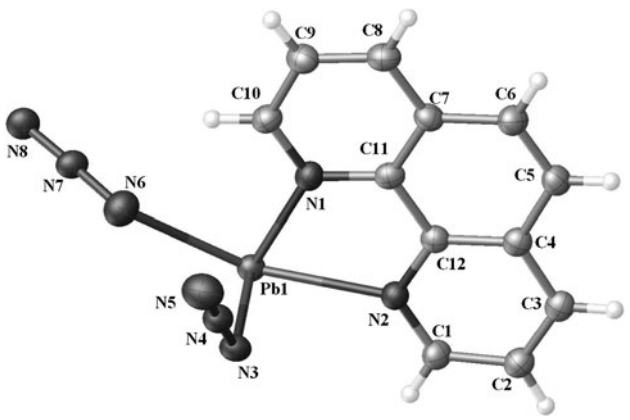

Fig. 3 The molecular structure of the asymmetric unit of **1**

The packing diagram of **1** exhibits a 3D supramolecular architecture arising from lone pair activity, π–π stacking, and a weak Pb···N interaction (Fig. 5). The structure exhibits fascinating self-assembled structural topologies via three different π–π stacking (edge-to-edge with a distance of 3.217 Å, face-to-face with a distance of 3.338 Å, and slipped face-to-face with a distance of 3.384 Å), which are appreciably shorter than normal π–π stacking [48, 49].

The calculated structural parameters are listed in Table 2. The significant figure is maintained at four, which is sufficient for one bond length to be differentiated from the other. It should be noted that the experimental data belong to the solid phase, whereas the calculated data correspond to the isolated molecule in the gas phase. However, the experimental and computational data in Table 2 clearly show that both sets of data differ only slightly from each other. For example, the largest difference between the experimental and calculated Pb1–N8^i length is about 0.102 Å, while the greatest deviation occurs in the N8^i–Pb1–N6 angle by ca. 3.85°. As a result, the calculated geometrical parameters represent a good approximation.

The Mulliken charges on lead(II) and the coordinated atoms were also calculated. The positive charge on lead(II) ions is 1.004. The considerably low positive charge on the lead(II) ion of **1** may be explained by its contribution to Pb···Pb interactions. The charges of the N atoms of the *o*-phen ligands were −0.688 and −0.630, respectively, while the N atoms of both azide anions (N6 and N3) had

Table 2 Selected bond lengths (Å) and angles [°] for [Pb(*o*-phen)($\mu_{1,1}$-N_3)($\mu_{1,3}$-N_3)]$_n$

	Experimental	Calculated
Pb1–N3	2.418(6)	2.403
Pb1–N8^i	2.816(5)	2.712
N2–Pb1	2.514(5)	2.496
N3^i–Pb1	2.706(5)	2.687
N6–Pb1	2.611(6)	2.590
N1–Pb1	2.502(5)	2.494
N1–Pb1–N3^i	79.59(16)	80.25
N3^i–Pb1–N6	119.84(19)	120.48
N8^i–Pb1–N6	104.66(19)	108.51
N8^i–Pb1–N3^i	131.71(19)	129.12
N3–Pb1–N2	79.70(18)	80.76
N6–Pb1–N2	80.43(19)	81.31
N3–Pb1–N1	81.75(18)	82.98
N2–Pb1–N1	66.18(17)	68.23
N3–Pb1–N3^i	69.8(2)	70.45
N3–Pb1–N6	77.6(2)	80.02

Symmetry transformations used to generate equivalent atoms: $i = -x, -y, -z$

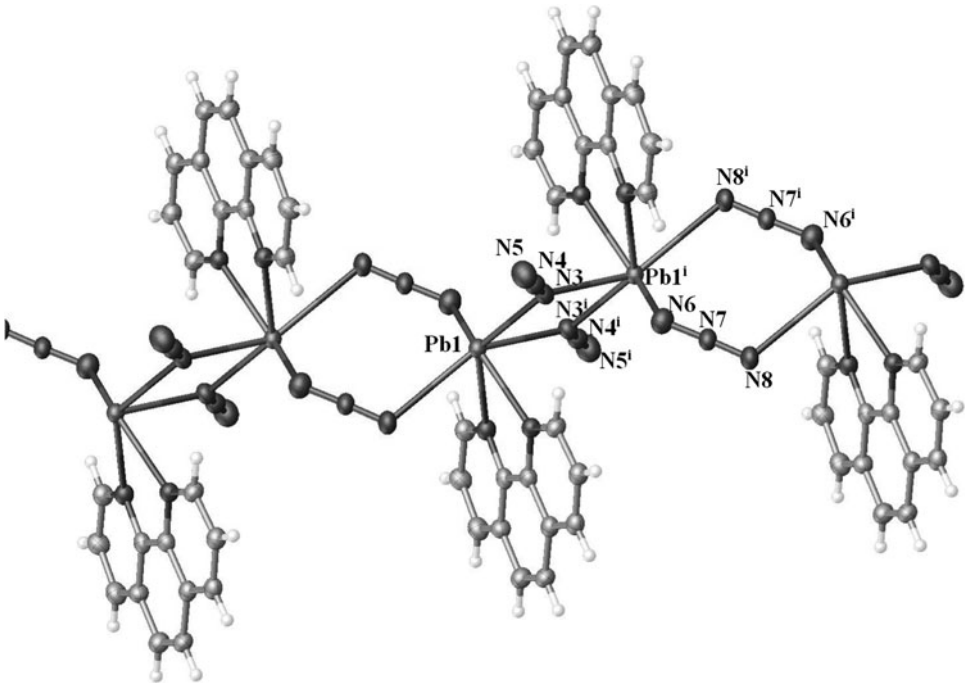

Fig. 4 Fragment of the 1D coordination polymer

similar charges: N6 = −0.540 and N3 = −0.535. The calculations indicate that **1** has 76 occupied molecular orbitals (MOs) for each [Pb(*o*-phen)($\mu_{1,1}$-N_3)($\mu_{1,3}$-N_3)] unit. The value of the energy separation between the highest occupied molecular orbital (HOMO) and the lowest unoccupied molecular orbital (LUMO) was calculated. Figure 6 shows the HOMO and LUMO for the lead(II) complex. The HOMO of the complex is principally

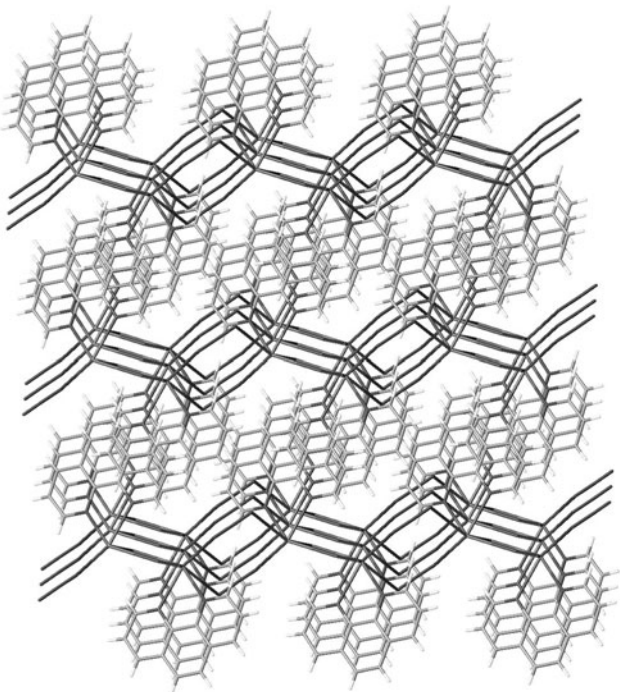

Fig. 5 Packing of the 1D chains to form a 3D supramolecular layer via π–π stacking interactions

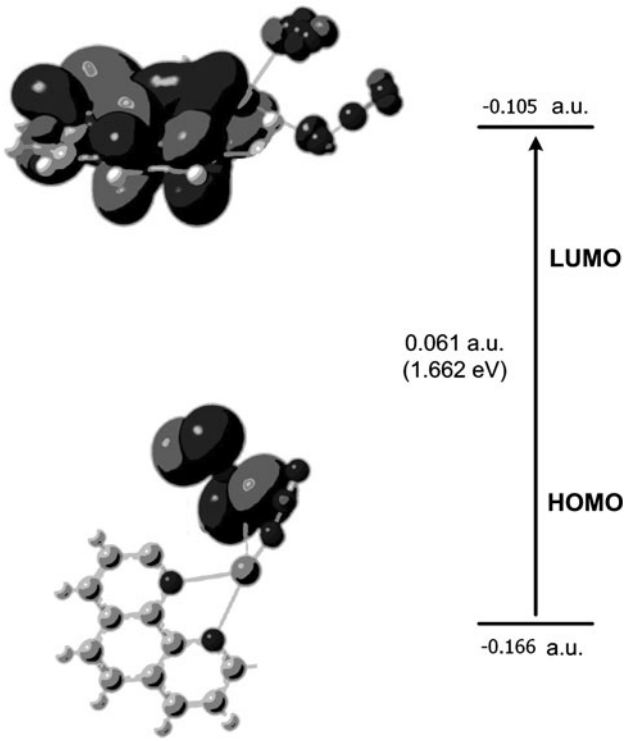

Fig. 6 Frontier molecular orbitals for a [Pb(*o*-phen)($\mu_{1,1}$-N_3)($\mu_{1,3}$-N_3)] unit

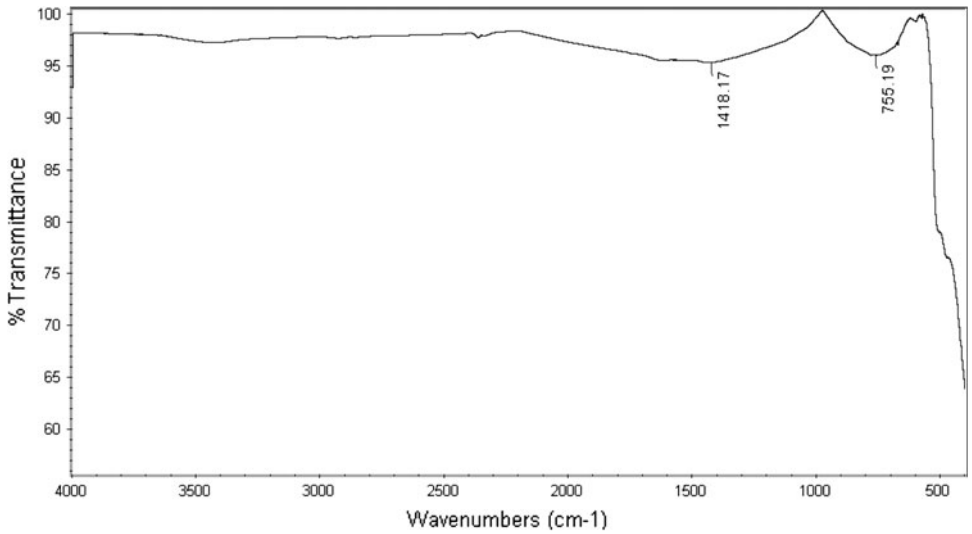

Fig. 7 FT-IR spectrum of nano-PbO after the calcination of **1**

localized among two N atoms of one azide anion, whereas the LUMO is delocalized approximately on all atoms of the *o*-phen ligand, including the lead(II) and azide anions. The calculated HOMO–LUMO gap is 0.061 a.u. (1.662 eV). In comparison with the lead azide ($Pb(N_3)_2$) gap (4.7 eV) [50], these studies found that the lead azide band gap is far larger than in **1**. Therefore, it can be expected that the complex is primary explosive and very sensitive to shock.

PbO powders were generated by the thermal decomposition of **1** in air. The elemental analysis contained no significant values for C, H and N. The IR spectra do not display characteristic organic absorption bands (Fig. 7). The powder XRD patterns (Fig. 8), which match the standard pattern of orthorhombic PbO with $a = 5.8931$ Å and $z = 4$ (JCPDS card file No. 77-1971), confirms the formation of PbO powder.

The significant broadening of the peaks of the nano structure indicates that the particles have nanometer dimensions. The average size of the particles was estimated by the Scherrer formula. The obtained value is $D = 35$ nm. The morphology and size of the prepared PbO samples were further investigated using SEM. The bulk powder of **1** produced regularly shaped

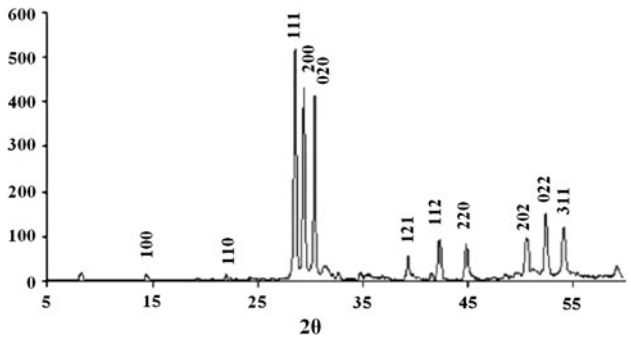

Fig. 8 XRD pattern of PbO after the calcination of **1**

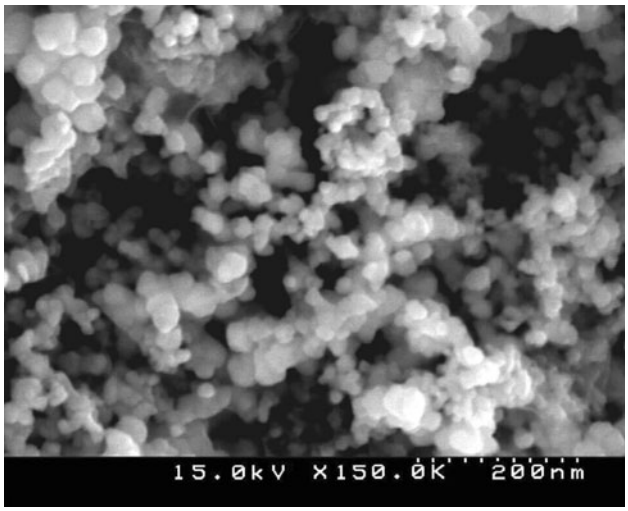

Fig. 9 SEM photograph of the PbO nano-powder produced by the calcination of **1**

Pb(II) oxide nanoparticles with a diameter of ~35 nm (Fig. 9), which is compatible to similar reports [51–57].

4 Conclusions

This work describes the construction of a novel 1D Pb(II) nano coordination polymer containing the Pb-($\mu_{1,1}$-N_3)($\mu_{1,3}$-N_3) unit with percent of aromatic amine (orthophenanthroline) and its use in the preparation of PbO nano-particles. The crystal structure of the complex was determined and indicates a one-dimensional polymer in the solid state. The arrangement of the ligands suggests a gap in the coordination geometry around the metal ions, possibly occupied by a

"stereoactive" lone pair of electrons on Pb(II). Two factors, lone pair activity and π–π stacking, may control the coordination sphere of Pb(II) ions in this complex. A theoretical study of the title complex was undertaken to examine the electronic structure and to obtain calculated bond distances and angles, which are in good agreement with the experimental data.

5 Supplementary Material

Crystallographic data for the structures reported in this paper have been deposited with the Cambridge Crystallographic Data Centre as supplementary publication CCDC-867597 for $[Pb(o\text{-phen})(\mu_{1,1}\text{-}N_3)(\mu_{1,3}\text{-}N_3)]_n$ (**1**). Copies of the data can be obtained upon application to CCDC, 12 Union Road, Cambridge CB2 1EZ, UK [Fax: +44-1223-336033; E-mail: de-posit@ccdc.cam.ac.uk].

Acknowledgments This work was supported by Grant No. RTI04-01-04 from the Regional Technology Innovation Program of the Ministry of Knowledge Economy (MKE).

References

1. A. Aslani, A. Morsali, M. Zeller, Solid State Sci. **10**, 1591 (2008); and references therein
2. H. Zhang, D.R. Yang, D.S. Li, X.Y. Ma, S.Z. Li, D.L. Que, Cryst. Growth Des. **5**, 547 (2005)
3. H.T. Shi, L.M. Qi, J.M. Ma, H.M. Cheng, J. Am. Chem. Soc. **125**, 3450 (2003)
4. F. Kim, S. Connor, H. Song, T. Kuykendall, P.D. Yang, Angew. Chem. Int. Ed. **43**, 3673 (2004)
5. D.B. Kuang, A.W. Xu, Y.P. Fang, H.Q. Liu, C. Frommen, D. Fenske, Adv. Mater. **15**, 1747 (2003)
6. A. Morsali, M.Y. Masoomi, Coord. Chem. Rev. **253**, 1882 (2009)
7. M. Fujita, Y.J. Kwon, O. Sasaki, K. Yamaguchi, K. Ogura, J. Am. Chem. Soc. **117**, 7287 (1995)
8. L.F. Mao, A. Mayr, Inorg. Chem. **35**, 3183 (1996)
9. K.-T. Wong, J.-M. Lehn, S.-M. Peng, G.-H. Lee, Chem. Commun. 2259 (2000)
10. J.S. Miller (ed.), *Extended Linear Chain Compounds*, vol. 1 (Plenum Press, New York, 1982)
11. M.A.M. Abu-Youssef, A. Escuer, D. Gatteschi, M.A.S. Goher, F.A. Mautner, R. Vicente, Inorg. Chem. **38**, 5716 (1999); and references therein
12. A. Caneschi, D. Gatteschi, N. Lalioti, C. Sangregorio, R. Sessoli, G. Venturi, A. Vindigni, A. Rettori, M.G. Pini, M.A. Novak, Angew. Chem. **40**, 1760 (2001)
13. A. Tanatani, M.J. Moi, J.S. Moore, J. Am. Chem. Soc. **123**, 1792 (2001)
14. Z.R. Ranjbar, A. Morsali, Ultrason. Sonochem. **18**, 644 (2011)
15. H. Sadeghzadeh, A. Morsali, CrystEngComm **12**, 370 (2010)
16. Z. Rashidi, A. Morsali, J. Mol. Struct. **936**, 206 (2009)
17. H. Ahmadzadi, F. Marandi, A. Morsali, J. Organomet. Chem. **694**, 3565 (2009)
18. H. Sadeghzadeh, A. Morsali, Ultrason. Sonochem. **18**, 80 (2011)
19. S.J. Tabatabaei Rezaei, M.R. Nabid, A. Yari, S. Weng Ng, Ultrason. Sonochem. **18**, 49 (2011)
20. Y. Hanifehpour, B. Mirtamizdoust, S.W. Joo, J. Inorg. Organomet. Polym Mater. **22**, 816 (2012)
21. Y. Hanifehpour, S. Mokhtari, B. Mirtamizdoust, S.W. Joo, J. Inorg. Organomet. Polym Mater. **22**, 923 (2012)
22. Y. Hanifehpour, B. Mirtamizdoust, S.W. Joo, J. Inorg. Organomet. Polym Mater. **22**, 916 (2012)
23. Y. Hanifehpour, B. Mirtamizdoust, S.W. Joo, J. Inorg. Organomet. Polym Mater. **22**, 549 (2012)
24. B. Mirtamizdoust, B. Shaabani, A. Khandar, H.-K. Fun, S. Huang, M. Shadman, P. Hojati-Lalemi, Z. Anorg. Allg. Chem. **638**, 844 (2012)
25. B. Shaabani, B. Mirtamizdoust, D. Viterbo, G. Croce, H. Hammud, P. Hojati-Lalemi, A. Khandar, Z. Anorg. Allg. Chem. **637**, 713 (2011)
26. M.Y. Masoomi, A. Morsali, Coord. Chem. Rev. **256**, 2921 (2012)
27. K.S. Suslick, S.B. Choe, A.A. Cichowlas, M.W. Grinstaff, Nature **353**, 414 (1991)
28. K.S. Suslick, in *Ultrasound: Its Chemical Physical and Biological Effect*, ed. by K.S. Suslick (VCH Publishers, Weinheim, 1989)
29. H. Chermette, Coord. Chem. Rev. **178**, 699 (1998)
30. Mercury 1.4.1, Copyright Cambridge Crystallographic Data Centre, 12 Union Road, Cambridge, CB2 1EZ, UK, 2001–2005
31. L.J. Farrugia, J. Appl. Crystallogr. **30**, 565 (1997)
32. A.D. Becke, J. Chem. Phys. **98**, 5648 (1993)
33. C. Lee, W. Yang, R.G. Parr, Phys. Rev. B **37**, 785 (1988)
34. P.J. Hay, W.R. Wadt, J. Chem. Phys. **82**, 270 (1985)
35. J.B. Foresman, A.E. Frisch. *Exploring Chemistry with Electronic Structure Methods,* 2nd edn. (Gaussian Inc.: Pittsburgh, 1996)
36. M. J. Frisch et al., *GAUSSIAN 98, Revision A.9* (Gaussian Inc., Pittsburgh, 1998)
37. K. Nakamoto, *Infrared and Raman Spectra of Inorganic and Coordination Compounds*, 5th edn., part B (Wiley, New York, 1997), pp. 124–126
38. M. Aoyagi, K. Biradha, M. Fujita, J. Am. Chem. Soc. **121**, 7457 (1999)
39. C.J. Holler, K. Muller-Buschbaum, Z. Anorg. Allg. Chem. **633**, 2614 (2007)
40. B. Wisser, Y. Lu, C. Janiak, Z. Anorg. Allg. Chem. **633**, 1189 (2007)
41. Y.X, Chi, S.Y. Niu, J.Jin, L.P. Sun, G. Di Yang, L. Ye, Z. Anorg. Allg. Chem. **633**, 1274 (2007)
42. B. Ding, J. Li, E.C. Yang, X.G. Wang, X.J. Zhao, Z. Anorg. Allg. Chem. **633**, 1062 (2007)
43. G. Mahmoudi, A. Morsali, L.G. Zhu, Z. Anorg. Allg. Chem. **633**, 539 (2007)
44. Y.Z. Tang, Y.H. Tan, S.H. Chen, Y.W. Chao, Z. Anorg. Allg. Chem. **633**, 332 (2007)
45. K. Abu-Shandi, H. Winkler, H. Paulsen, R. Glaum, B. Wu, C. Janiak, Z. Anorg. Allg. Chem. **631**, 2705 (2005)
46. L. Shimoni-Livny, J.P. Glusker, C.W. Brock, Inorg. Chem. **37**, 1853 (1998)
47. R.D. Hancock, M.S. Shaikjee, S.M. Dobson, J.C.A. Boeyens, Inorg. Chim. Acta **154**, 229 (1998)
48. C.A. Hunter, J.K.M. Sanders, J. Am. Chem. Soc. **112**, 5525 (1990)
49. C. Janiak, J. Chem. Soc. Dalton Trans. 3885 (2000)
50. E.H. Younk, A.B. Kunz, Int. J. Quantum Chem. **63**, 615 (1997)
51. K. Akhbari, A. Morsali, CrystEngComm **13**, 2047 (2011)
52. L. Hashemi, A. Morsali, P. Retailleau, Inorg. Chim. Acta **367**, 207 (2011)
53. G. Shahverdizadeh, F. Hakimi, B. Mirtamizdoust, A.A. Soudi, P. Hojati-Talemi, J. Inorg. Organomet. Polym. **22**, 903 (2012)
54. L. Aboutorabi, A. Morsali, Ultrason. Sonochem. **18**, 407 (2011)
55. M.J. Soltanian Fard, A. Morsali, J. Inorg. Organomet. Polym. Mater. **20**, 727 (2010)
56. L. Hashemi, A. Morsali, J. Inorg. Organomet. Polym. **20**, 856 (2010)
57. H. Sadeghzadeh, A. Morsali, J. Inorg. Organomet. Polym Mater. **20**, 733 (2010)